16th World Conference on Earthquake, 16WCEE 2017

Santiago Chile, January 9th to 13th 2017

Paper N° 1714 (Abstract ID)

Registration Code: S-E1463220262

IMPROVEMENT OF ENERGY TRANSMITTING BOUNDARY FOR THREE DIMENSIONAL NONLINEAR ANALYSIS

Naohiro Nakamura[1]

[1] *Professor, Graduate Scholl of Engineering, Hiroshima University, naohiro3@hiroshima-u.ac.jp*

Abstract

It is important to consider both the soil-structure interaction and nonlinear effects to accurately estimate the behavior of buildings during severe earthquakes. In addition, three dimensional (3D) models are needed to express the complex shape of buildings, basements, and piles. In recent years, large scale 3D time history nonlinear analyses using the finite element method (FEM) have been performed.

Although the soil has a semi-infinite extent, a soil model needs to be generated as a finite region model in FEM analyses. Therefore, artificial wave boundary models are needed. Currently, simple models such as the cyclic boundary or the viscous boundary are often used mainly as the side wave boundary model. These simple models are simple to use but do not provide high accuracy. As a result, the wave boundary cannot be placed close to the analysis object, and the analysis modeling domain size and analysis load are enlarged. For this reason, it is desirable to improve the wave boundary accuracy and reduce the analysis domain size.

Although the energy transmitting boundary is accurate and efficient for FEM earthquake response analysis, it can only be applied in the frequency domain. The author proposed the time domain transmitting boundary by applying a new method that can transform the frequency dependent function into the time domain. By using this time domain transmitting boundary, time domain analysis became possible. In this method, the analysis model can be divided into three parts: the inner field, the outer field, and the boundary itself. In the first paper, two in-plane problems were proposed. In the study, only the inner field can be treated as a nonlinear system. In the next study, the outer field and the boundary itself can be treated as a nonlinear system. In addition, a model was also proposed.

In a previous study, this technique was expanded for 3D problems. The inner field is supposed to be hexahedron-shaped and the approximate time domain boundary was set around it. The boundary comprised two parts. One was the 2D in-plane time domain boundary and the other was the anti-plane time domain boundary. The efficiency of the proposed method was confirmed using some example problems.

In this paper, based on these studies, 3D energy transmitting boundaries for nonlinear analyses are studied. First, an outline of the 3D transmitting boundary is provided. Then, improvements of the boundary for nonlinear problems are also explained. The efficiency of the proposed method was studied by comparison with a conventional viscous boundary. As a result, the efficiency of the proposed method was confirmed.

Keywords: Transmitting boundary, 3 Dimensional FEM, Time domain, Seismic Response Analysis, Nonlinear Analysis

1. Introduction

Considering both soil-structure interaction and nonlinear effects is important to accurately estimate the behavior of buildings during severe earthquakes. In addition, three dimensional (hereafter referred to as “3D”) models are needed to express the complex shape of buildings, basements, and piles. In recent years, large scale 3D time history nonlinear analyses using the finite element method (FEM) have been performed.

Although the soil has a semi-infinite extent, a soil model needs to be generated as a finite region model in FEM analyses. Therefore, artificial wave boundary models are needed, especially, at the side of the soil model. Currently, simple models such as the cyclic boundary or the viscous boundary [1] are often used mainly as the side wave boundary model. They are simple to use, but their accuracy is not high. As a result, the wave boundary cannot be placed close to the analysis object, and the analysis modeling domain size and analysis load are enlarged. For this reason, it is desirable to improve the wave boundary accuracy and reduce the analysis domain size (see Fig. 1).

Many investigations into this problem have been conducted, e.g., [2-10]. Although there were certain results from these studies, limited application examples have been presented. Therefore, more practical methods for actual complex problems are needed.

In contrast, the energy transmitting boundary (hereinafter referred to as “TB”) used in FLUSH [11] and ALUSH [12] is a highly accurate and efficient side wave boundary. However, TB can only be applied to frequency domain linear analysis and equivalent linear analysis, e.g., [13]. It is possible to significantly reduce the analysis load for 3D time history FEM analysis by transforming TB to the time domain.

The author has previously proposed time domain transform methods of strongly frequency dependent dynamic stiffness, and proved that these methods are accurate yet simple [14]. As an application of the methods, TB for a two dimensional (2D) in-plane problem that corresponds to FLUSH was transformed to a time domain. It was confirmed that highly accurate analyses in the time domain are also possible, as in the frequency domain. Then, nonlinear response of an inner field building was calculated and favorable results were obtained [15]. A study was also conducted to consider the semi-infinite condition at the bottom of TB [16]. Furthermore, a 2D nonlinear transmitting boundary was studied and proposed [17]. By using it, all of the inner field, the outer field, and the boundary itself can be treated as a nonlinear system.

In a previous paper [18], 3D time history FEM analyses with TB were studied based on these results. The axisymmetric boundary model used in ALUSH is known as a 3D problem TB. However, in many cases, the orthogonal coordinate system is preferred to the axisymmetric coordinate system for actual problems, as shown in Fig. 1. Therefore, in this paper, the orthogonal coordinate system is used for modeling of the inner field (see Table 1). Accordingly, the TB should also be formulated using orthogonal coordinates rather than axisymmetric coordinates, but it is not possible to obtain such a theoretical solution. Therefore, an approximate 3D boundary model (hereinafter referred to as the 3D-TB model) from a combination of a 2D in-plane problem TB corresponding to FLUSH [11] (hereinafter referred to as SV-TB) and a 2D anti-plane problem TB [19] (hereinafter referred to as SH-TB) was used.

In this paper, improvement of the boundary for 3D nonlinear problems is studied. The building, the soil, and the boundary itself are thought to be nonlinear. First, an outline of the 3D-TB model for linear analyses used in a previous paper [18] is shown. Next, a method to improve the boundary for nonlinear analyses is explained.

Then, nonlinear response analysis of the 3D soil-structure interaction system using the proposed 3D-TB model is conducted and the efficiency of the model is evaluated.

The viscous boundary (hereinafter referred to as VB), which is currently thought to be the most practical method for time domain analysis, was used for comparison in this study.

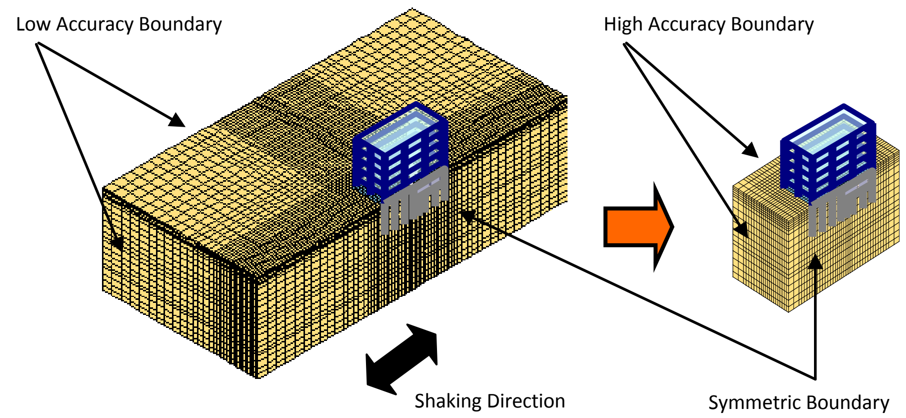

Fig. 1 – Reduction of the analysis region of the inner field with a high accuracy boundary.

Table 1 – Shape of the inner field and type of TB.

Shape of the Inner Field	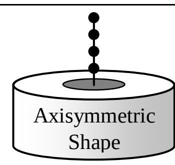	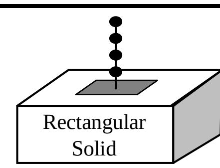
Coordinate System	Axisymmetric	Orthogonal
Transmitting Boundary	Theoretical Method	Approximate Method (Proposed Method)

2. Outline of 3 Dimensional Transmitting Boundary in the time domain

The TB is a highly accurate boundary model located at the outer side of the inner soil model, which is formed by parallel layers on the rigid bedrock. In a horizontal direction, the formulation is theoretical and rigorous. In a vertical direction, the formulation is approximate since it follows the element displacement assumption. The TB is able to almost completely absorb wave motion from an arbitrary direction. Even when the bottom of the soil is in a semi-infinite condition, a favorable evaluation is possible by adding a sufficient amount of elements to the soil bottom in the frequency domain.

In this paper, a time domain 3D-TB model, which corresponds to an orthogonal coordinate system and uses SV-TB and SH-TB approximately, is proposed. An outline of this is described hereinafter.

2.1 Image of the 3D transmitting boundary

An image of an inner field model is shown in Fig. 2. In the figure, a vertical nodal group (hereinafter referred to as a “nodal line”) is considered on the boundary surface. This is placed as a basic unit to form the boundary model. The boundary surface is expressed as a collection of these nodal lines.

The control width of one nodal line extends to the center of the adjacent nodal lines. Both SV-TB and SH-TB are assigned in this nodal line (refer to Fig. 3). Therefore, the degree of freedom within a nodal line is coupled, but the degree of freedom with the other nodal lines is not coupled. Theoretically, all nodal lines should be coupled with each other, but in the proposed model, the efficiency of the calculation is improved by disregarding this.

Furthermore, if the soil properties are the same, each nodal line becomes a TB with identical properties, and only the control width is different. For this reason, a TB with a unit width nodal line that corresponds to the type of soil properties is prepared. This is multiplied by the control width and assigned to the entire boundary surface. The analysis flow is shown in Fig. 4. The SH-TB and SV-TB are calculated in the frequency domain. These TB matrices are transformed to the time domains and assigned to the overall equation of motion.

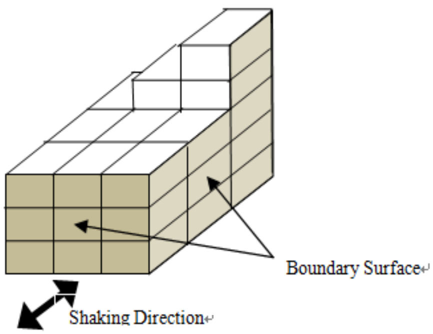

Fig. 2 – Image of the inner field.

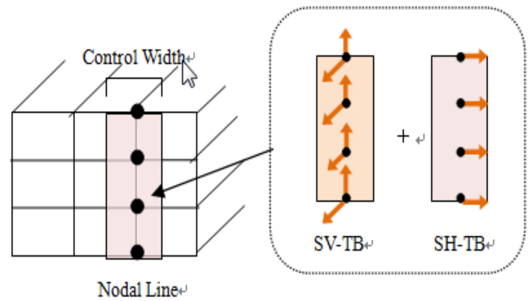

Fig. 3 – Assignments of SV-TB and SH-TB to a nodal line.

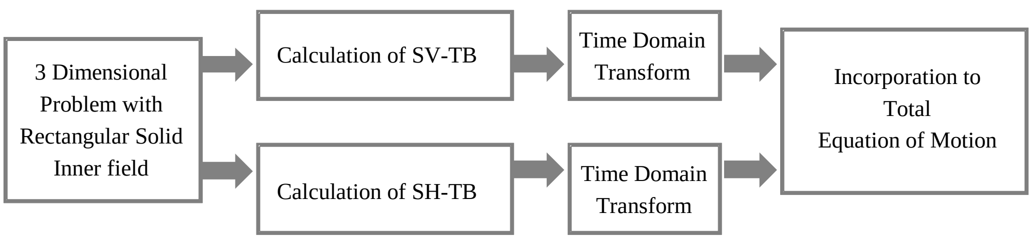

Fig. 4 – Analysis flow.

2.2 Transformation of TB matrices to the time domain

The reaction force from TB has to be calculated in the time domain. The calculation is not easy because the components of the TB matrix are strongly frequency dependent. In this section, the concept of the transformation of TB to the time domain and the obtained reaction force in the time domain will be briefly explained using a simple single DOF equation.

Although many methods for transforming the frequency dependent impedance function to the time domain have been proposed, most of them employed either the past displacement or the past velocity in the formulation of the impulse response. The author proposed transform methods using both the past displacement and velocity, and then confirmed that the accuracy of these methods are high [20,21].

In this paper, the following methods were used for the transform. Here, Eq. (1) in the frequency domain is considered. $Y(\omega)$ is the reaction force, $H(\omega)$ is the frequency dependent function (this corresponds to TB), and $x(\omega)$ is the displacement. The objective is to obtain the reaction force in the time domain $y(t)$. In the proposed methods, $Y(\omega)$ and $H(\omega)$ are approximated by $Y'_B(\omega)$ and $H'_B(\omega)$, as shown in Eq. (2). This equation is expressed as Eq. (3) in the time domain, where $y'_B(t)$ and $x(t)$ are the reaction force and the displacement in the time domain.

$$Y(\omega) = H(\omega) \cdot x(\omega) \qquad (1)$$

$$Y'_B(\omega) = H'_B(\omega)\cdot x(\omega) = \left(\sum_{j=0}^{n'} {}_0h_j \cdot e^{-i\omega t_j} + i\omega\cdot\sum_{j=0}^{n'} {}_1h_j \cdot e^{-i\omega t_j} - \omega^2 \cdot {}_2h_0\right)\cdot x(\omega) \tag{2}$$

$$y'_B(t) = \sum_{j=0}^{n'} {}_0h_j \cdot x(t-t_j) + \sum_{j=0}^{n'} {}_1h_j \cdot \dot{x}(t-t_j) + {}_2h_0 \cdot \ddot{x}(t) \tag{3}$$

$t_j = j\Delta t$, where Δt is the discrete time interval for the transform. ${}_0h_j$, ${}_1h_j$, and, ${}_2h_0$ are the coefficients of the impulse response. ${}_0h_0$, ${}_1h_0$, and ${}_2h_0$ are called the simultaneous components because they correspond to the current time t. ${}_1h_1 \sim {}_1h_{n'}$ and ${}_0h_1 \sim {}_0h_{n'}$ are called the time-delay components since they correspond to the past time $(t - t_j)$. All of the unknown coefficients of the impulse response are obtained from simultaneous equations with given function data for $H(\omega i)$ ($I = 0,1,2,\ldots N$). This method is called method B'.

In the case when the hysteretic damping is large, the accuracy of the transform tends to decrease. To improve this problem, the simultaneous components (${}_2h_0$, ${}_1h_0$, ${}_0h_0$) are corrected with (Δ_2h_0, Δ_1h_0, Δ_0h_0), where Δ_2h_0, Δ_1h_0, and Δ_0h_0 indicate the modification terms determined using the least squares method. The improved reaction force ($Y_C(t)$ and $y_C(\omega)$) can be expressed using Eqs. (4) and (5). This method is called method C'. Using Eqs. (4) and (5), all the components of $[T_B]$ can be transformed to the time domain. Details of the transformation is presented in Nakamura (2007, 2012a).

$$Y'_C(t) = \left(H'_B(\omega) - \omega^2 \cdot \Delta_2h_0 + i\omega\cdot\Delta_1h_0 + \Delta_0h_0\right)\cdot x(\omega) \tag{4}$$

$$y'_C(t) = y'_B(t) + \left(\Delta_0h_0 \cdot x(t) + \Delta_1h_0 \cdot \dot{x}(t) + \Delta_2h_0 \cdot \ddot{x}(t)\right) \tag{5}$$

3. Improvement for nonlinear analysis

In a previous paper, it was possible to consider the nonlinear characteristic for the inner field, but it was necessary to treat the outer field (free field) and TB as linear or an equivalent linear form. In this paper, it is possible to consider the nonlinear characteristic for outer field objects as well as TB, and a seismic response analysis method is proposed that considers the entire analysis model as nonlinear (see Table 2).

Table 2 – Method proposed in this paper.

	Outer field	TB	Inner field
Frequency Domain TB	L	L	L
Time Domain TB	L	L	N
Proposed Method	**N**	**N**	**N**

*) L: linear or equivalent linear, N: nonlinear

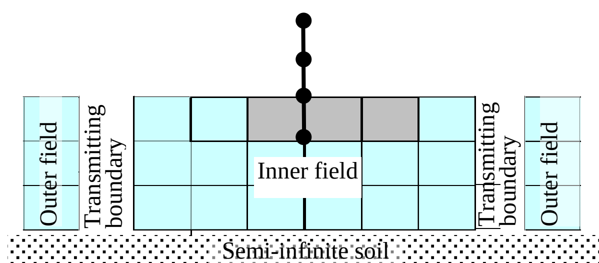

Fig. 5 – Simple image of the analysis model.

In seismic response analysis that uses TB, the analysis region can be divided into three sections as shown in Fig. 5: (1) outer field, (2) inner field, (3) TB. Hereafter, the outlines of the nonlinear response analysis method used nonlinear TB for each of these three sections.

3.1 Outer field

The outer field is distant from the inner field and represents parallel layered soil (free field) which has a sufficient spread. In order to be consistent with the analysis result of the inner field, a 1-dimensional wave propagation analysis is performed using a vertical column soil model with solid elements. The depth direction of the model is split and the physical soil properties are the same as the outermost edge of the inner field. The nonlinear analysis is performed using the same solid elements as the outermost edge of the inner field. Physical properties of each element are considered to change based on the given dynamic deformation characteristics (G-γ, h-γ relationship). Here, G is the shear modulus, h is the damping ratio, and γ is the shear strain.

In this paper, a nonlinear causal hysteretic damping model [20] is used for the soil analysis. This is a model where the stiffness and damping changes at each time step under the condition that the damping ratio is almost constant in a certain frequency range. The shear modulus and damping ratio changes at each time step, depending on the maximum shear strain of the previous Δt_m second. In this paper, $\Delta t_m = 1$ is used.

3.2 Inner field

The inner field consists of the building, the foundation, and soil in the vicinity of them. In this paper, the building is represented by a lumped mass model with a shear element. The restoring force characteristics are set for each member, and time history nonlinear responses analysis is performed.

The soil, as with the outer field, is modeled using solid elements, and the nonlinear characteristics of every moment is evaluated using the nonlinear causal hysteretic damping model based on the given G-γ, h-γ relationship. For the shear strain, the main shear strain (γ_1) of Eq. (6) is used, where ε_1 and ε_3 are the maximum principal shear strain and the minimum principal shear strain, respectively. It is the expanded equation used in [17] from 2D to 3D. The shear modulus and damping ratio are varied according to the maximum principal shear strain (γ_{1max}) of the previous 1 second. For this analysis, the Poisson's ratio does not change even after nonlinear deformation. As a result, the Young's modulus of each element changes with the same ratio as the shear modulus.

$$\gamma_1 = \varepsilon_1(t) - \varepsilon_3(t) \tag{6}$$

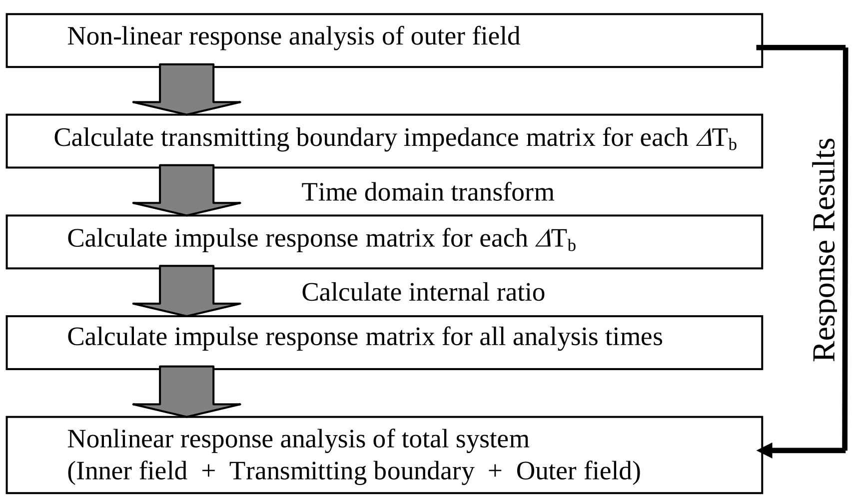

Fig. 6 – A flow chart of earthquake response analysis using a non-linear transmitting boundary.

3.3 TB

TB is also changed depending on the change in the physical properties of the outer field. However, calculating the impedance matrices of SH-TB and SV-TB for each ΔT (analysis time step) is likely to incur a large computational load. Therefore, for a certain time interval (hereinafter referred to as ΔT_b), TB is calculated using the physical properties of that time, and is also interpolated during that time. More specifically, the calculation is performed as follows (see Fig. 5). In this paper, ΔT_b was set to 1 second and ΔT was set to 0.01 seconds. If ΔT_b is decreased to ΔT, it becomes the same as calculating the TB matrix for each analysis time.

(1) First the outer field is calculated, and the physical soil properties are determined for each time ΔT_b (0, ΔT_b,

$2\Delta T_b$, $3\Delta T_b$, ...).

(2) Using the physical soil properties, the impedance matrix of TB for each ΔT_b is calculated.

(3) The components of the matrix for each ΔT_b are transformed to the time domain, and the impulse response matrix is calculated. In addition, the time domain transformation method is the same as in [17].

(4) The parameters that control the interpolation of TB are selected. In this paper, the element that has the maximum shear strain in the outer field is selected, and the shear strain value of that element at each time is used as the control parameter (hereinafter, γ_{Emax} (t)).

(5) Let us assume that the current time (hereinafter referred to as t) is between j ΔT_b and (j+1) ΔT_b. First, we solve the ratio γ_{Emax}(t), and internally divide γ_{Emax} (jΔT_b) and γ_{Emax} ((j+1) ΔT_b). The impulse response matrix at time t has the same ratio as above, and is used to internally divide the impulse response matrix of jΔT_b and (j+1) ΔT_b. The impulse response matrix for all analysis times is thereby calculated.

3.4 Nonlinear causal hysteretic damping model

In time history earthquake response analysis of the inner field and the outer field, the causal hysteretic damping model [20] is used in the same manner as [17] as a way to represent the frequency-independence of material damping. The applicability of the causal hysteretic damping model to the nonlinear element has been previously confirmed in [17]. Equation (7) shows the relational expression of element displacement - element force of the time domain using the nonlinear causal hysteretic damping model. This is almost the same as in a previous study. In this paper, however, to take into account the nonlinear characteristics of the element, the time change is represented by (t) attached to [K_e(t)], which is the element stiffness matrix, and h_e(t) is the element damping ratio. Also, {F_e} and {u_e} are the element force vector and the element displacement vector, respectively. The damping force is calculated by the damping term's simultaneous component (c_0) and the stiffness term's time delay component (k_1, k_2 ,... k_n), where k_j = k(jΔt_d). As indicated in a previous study, the study frequency range was set as 0 – 10 Hz, Δt_d = 0.05 s, and the 18-term model [20] was used.

$$\{F_e(t)\} = [K_e(t)\ ]\left[\{u_e(t)\} + 2h_e(t)\left(c_0\{\dot{u}_e(t)\} + \sum_{j=1}^{n} k_j\{u_e(t-t_j)\}\right)\right] \tag{7}$$

4. Example problems

4.1 Analysis models and conditions

The analysis model is shown in Fig. 7. Figure 8 shows an example of several models. For comparison, the distance L from the outer edge of the building to the boundary was set as 5, 10, 20, 40, 60, 80, or 100 m. Both the soil and building have nonlinear characteristics. The material properties of the soil and the building are shown in Tables 3 and 4, respectively. The initial damping ratio was set to 3% for the building and 2% for the soil, and the causal hysteretic damping model [20] was used. The soil consisted of a surface layer and base rock. In the surface layer, the thickness was 40 m, the shear velocity was in the range 200 to 400 m/s, and the nonlinear characteristics were considered based on the G-γ, h-γ relationship shown in Fig. 9. A height difference of 10 m was set for one side of the soil (only the left side). The shear velocity of the bedrock was 500 m/s. The bedrock was evaluated using the bottom VB in the inner field.

The building had six floors and was represented by a lumped mass model with shear elements. Its width was 20 m, the height of the above-ground part was 24 m, and the height of the rigid basement part was 10 m. Figure 10 shows the skeleton curve of each floor of the building. The shear force of the first folding point and second folding point of each curve were set to correspond to a static seismic intensity of 0.3 and 1.0, respectively. The normal tri-linear type was used for the hysteresis loop of each floor.

The input ground motion was the El Centro 1940NS wave (duration of 10 s, time step ΔT of 0.01 s), with the maximum acceleration set to 500 Gal and defined as 2E (double the ascending wave) at the bottom VB. For the time integral method, the Newmark-β method (β = 1/4) was used.

The study was performed for two cases. Case T used the nonlinear TB proposed in this paper. Case V used the conventional VB. For both Case TB and Case V, nonlinear calculations were used for the inner field and the outer field. The calculation of the boundary for Case T was nonlinear, while that for Case V was equivalent linear analysis using SHAKE [22]. The effect of the width of the inner field (L) on the accuracy was investigated for each case.

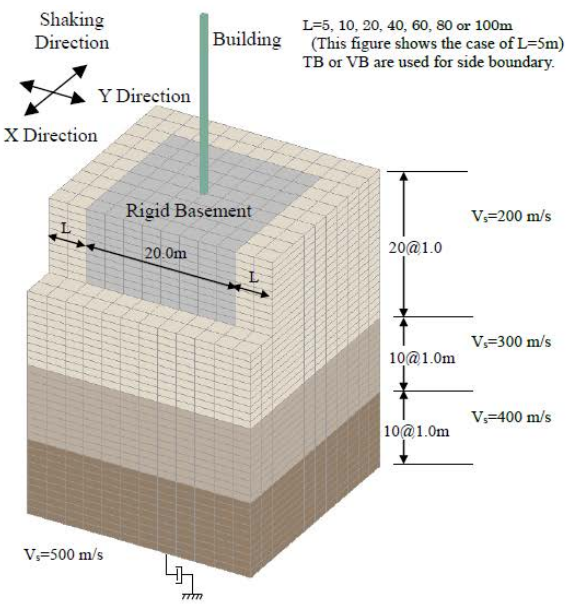

Fig. 7 – Analysis model in detail

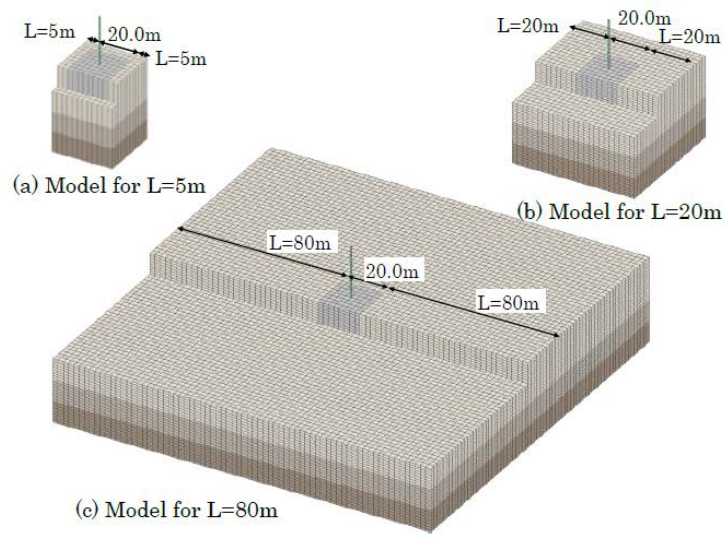

Fig. 8 – Example of models: (a) L = 5 m, (b) L = 20 m, (c) L = 80 m

Table 3 – Properties of the soil

	V_s (m/s)	Poisson Ratio ν	density ρ(t/m³)	Damping Ratio h	Thickness (m)
Surface1	200	0.4	2.0	0.02	20
2	300				10
3	400				10
Bedrock	500			0	-

Table 4 – Properties of the building

Story	Height (m)	Weight (t)	Rotational Inertia ($\times 10^5$tm²)	Shear Stiffness ($\times 10^6$kN/m)
6	4.0	480	0	0.4935
5	4.0	480	0	0.9047
4	4.0	480	0	1.234
3	4.0	480	0	1.480
2	4.0	480	0	1.645
1	4.0	480	0	1.727
B1	5.0	720	0	∞
B2	5.0	720	1.68	∞

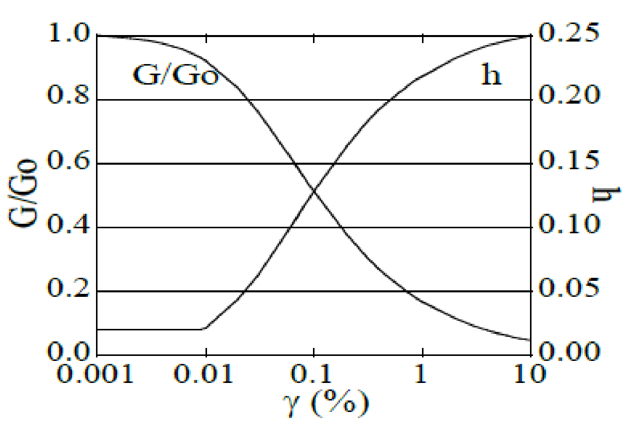

Fig. 9 – Dynamic deformation characteristics of the soil

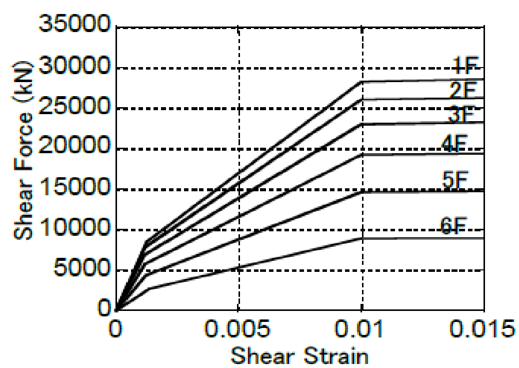

Fig. 10 – Building skeleton curves

4.2 Calculation of the outer field

Figure 11 indicates the shear strain time history waveform of the representative position (GL-19.5 m) of the outer field. As shown in the previous section, Δt_m = 1.0 s was used. According to γ of Δt_m = 1.0 s, the shear modulus G and the damping ratio h changed based on the G-γ, h-γ relationship. The TB matrix of the frequency domain was calculated using the physical properties at each ΔT_b. In this paper, ΔT_b = 1 s was used.

Figure 12 shows the distribution of the shear strain, Vs (shear wave velocity), and h (damping ratio) calculated from the G-γ, h-γ relationship at representative times (1, 3, 8 s). Accordingly, the TB matrix of the frequency domain corresponding to the soil's physical properties was calculated for each time. Frequency analysis was carried out over the range of 0.5 to 20 Hz in 0.5 Hz increments. From here, the TB matrix was obtained as a frequency-dependent complex matrix for each ΔT_b and this result was used for every case.

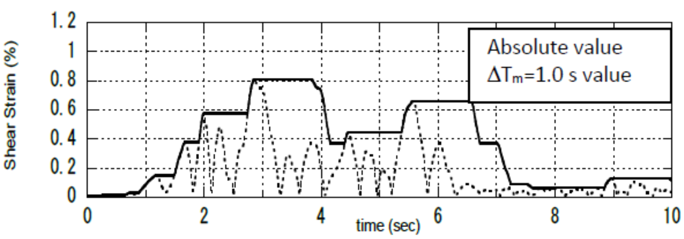

Fig. 11 – Shear strain time history of the representative position (GL-19.5 m) of the outer field

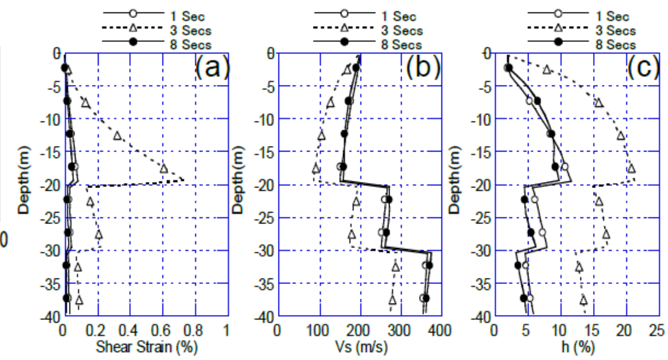

Fig. 12 – Representative time distribution, (a) shear strain, (b) shear wave velocity, and (c) damping ratio

4.3 Comparison of building response

Figure 13 shows the horizontal maximum response values (acceleration, displacement, and shear force) for the above-ground part of the building for Case V in the x direction. In the figure, three cases (L = 5, 40, and 100 m) are compared. The results for Case T at L = 100 m, which are thought to be the most accurate among all cases (hereafter referred as "the high-accuracy values"), are also shown in this figure. The results for VB at L = 100 m almost correspond with the high-accuracy values, but the results at L = 5 m and L = 40 m are significantly different from the high-accuracy values.

Figure 14 shows the maximum values for Case T in the x direction. Although there are slight differences in some parts of the acceleration values and shear force values between L = 5 m and the other cases, the results for all cases generally correspond favorably. Regarding the results for the y direction for Case V and Case T, both tendencies are almost the same as for the x direction.

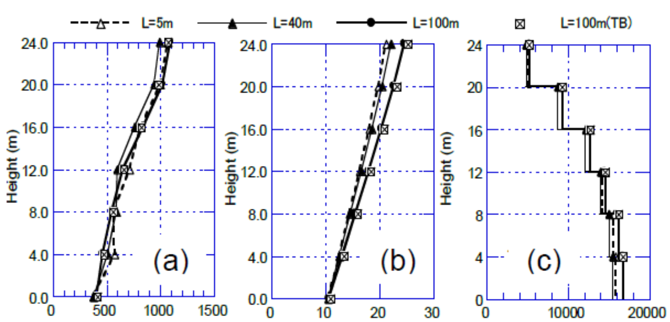

Fig. 13 – Comparison of the maximum response value of the building (Case V, x direction). (a) Maximum response acceleration (Gal), (b) maximum response displacement (cm), and (c) maximum shear force (kN)

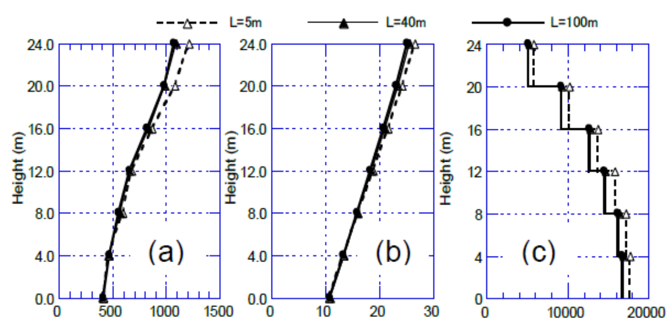

Fig. 14 – Comparison of the maximum response value of the building (Case T, x direction). (a) Maximum response acceleration (Gal), (b) maximum response displacement (cm), and (c) maximum shear force (kN)

Table 5(a) shows the ratios of these maximum values for Case V and the high-accuracy values. The black fields in the table indicate where the maximum difference exceeded 20% and the gray fields indicate where the maximum difference ranged from 10 to 20%. The differences exceeded 20% for some fields in the case of L = 5 m, and exceeded 10% for some fields in the case of L = 60 m. Table 5(b) shows the ratios for Case T. The differences exceeded 10% in some fields in the cases of L = 5 m and L = 10 m. From the comparison results, it can be said that the accuracy of Case V and Case T was favorable at L = 80 m and L = 20 m, respectively, since all differences were less than 10%.

Table 5 – Comparison of maximum response of the building

(a) Case V

Model	Excitation	Acceleration	Displacement	Shear force
L = 5 m	X	0.90-1.21	0.84-0.96	0.94-1.02
	Y	0.78-1.04	0.94-1.03	0.92-0.97
L = 40 m	X	0.90-1.07	0.88-0.97	0.93-0.96
	Y	0.84-1.08	0.85-1.02	0.86-0.91
L = 60 m	X	0.94-1.17	0.93-0.96	0.98-1.01
	Y	0.92-0.98	0.89-1.00	0.95-0.97
L = 80 m	X	0.96-1.05	0.96-0.97	1.00-1.01
	Y	0.94-1.04	0.94-0.98	0.99-0.99
L = 100 m	X	0.98-1.04	0.97-0.98	1.00-1.02
	Y	0.98-1.02	0.98-0.98	1.00-1.01

(b) Case T

Model	Excitation	Acceleration	Displacement	Shear force
L = 5 m	X	0.96-1.13	0.98-1.06	1.06-1.13
	Y	0.92-1.02	1.00-1.01	1.00-1.01
L = 10 m	X	0.97-1.12	0.98-1.05	1.06-1.12
	Y	0.95-1.02	1.00-1.00	1.00-1.01
L = 20 m	X	0.96-1.09	0.99-1.04	1.05-1.08
	Y	0.94-1.00	1.00-1.00	0.98-0.99
L = 40 m	X	0.98-1.03	1.00-1.02	1.01-1.02
	Y	0.97-1.05	0.99-1.01	0.98-0.99

*1) Values in these tables show the range of maximum responses (as ratios to the response of TB, L = 100 m).
*2) The color of each field shows the maximum difference (black: more than 20%, gray: between 10% to 20%, and white: less than or equal to 10%).

Table 6 – Comparison of analysis loads (cases whose differences in building response were less than 10%)

Model	L (m)	No. of Node	No. of Elem	Required memory (GB)	Analysis time (min)
V	80 m (4.0)	195,135 (8.3)	184,336 (8.7)	18.0 (6.4)	628 (5.7)
T	20 m	23,631	21,136	2.8	110

*1) The values in the parenthesis mean the magnification to TB.

Table 6 provides a comparison of the analysis loads for the cases that exhibited favorable horizontal response results for the building in Table 5, with L = 20 m for Case T and L = 80 m for Case V. As for the analysis load, the required memory size and the analysis time during the calculations were counted using a single core Xeon 7560 (2.26 GHz) processor. This processing unit had 256 GB of main memory space and the calculations for all cases were conducted within the main memory. Furthermore, the 3D-TB calculation time in the frequency domain and the time domain transformation time (the total for both for the SV problem and the SH problem was 13 minutes) were included in the TB analysis time.

Compared to Case V, Case T had around 1/8 of the number of inner field nodal points and elements. It also required approximately 1/6 of the memory and analysis time. Compared to the results of linear TB (1/30 of the number of inner field nodal points and elements and 1/13 of the required memory and analysis time) [18], the effect of nonlinear TB is not the same; however, it is still efficient.

5. Conclusions

In this paper, a nonlinear transmitting boundary for 3D problems was proposed. From the results of the example analysis, it was confirmed that the accuracy and the efficiency of the model are high.

6. Acknowledgements

This work was supported by JSPS KAKENHI Grant Number 26289197.

7. References

[1] Lysmer, J. and Kuhlelameyer, R.L. (1969). Finite dynamic model for infinite area. *J. Eng. Mech. Div., ASCE*, 95(3), 859-877.

[2] Smith,W. (1973). A Non-reflecting Plane Boundary for Wave Propagation Problems. *J. Computational Physics*, 15: 492-503

[3] Kim, D.K. and Yun, C.B. (2000). Time Domain Soil-Structure Interaction Analysis in Two-Dimensional Medium Based on Analytical Frequency-Dependent Infinite Elements. *Engineering Structures*, 22(3), 258-271

[4] Wolf, J.P. and Song, C. (1996). *Finite-Element Modelling of Unbounded Media*. John Wiley & Sons Ltd, West Sussex, England

[5] Wolf, J.P. (2003). *The Scaled Boundary Finite Element Method*. John Wiley & Sons Ltd, West Sussex, England

[6] Berenger, J.P. (1994). A Perfectly Matched Layer for the Absorption of Electromagnetic Wave. *J. Computational Physics*, 114(2), 185-200

[7] Hastings, F.D. Schneider, J.B. and Broschat, S.L. (1996). Application of the Perfectly Matched Layer (PML) Absorbing Boundary Condition to Elastic Wave Propagation. *J. Acoustical Society of America*, 100(5), 3061-3069

[8] Basu, U. and Chopra, A.K. (2004). Perfectly matched layers for transient elastodynamics of unbounded domains. *Int. J. Numerical Methods in Engineering*, 59, 1039–1074

[9] Millan, M, A. and Dominguez, J. (2009). Simplified BEM/FEM Model for Dynamic Analisis of Structures on piles and Pile Group in Viscoelastic and Poroelastic soils. *Eng. Anal. Bound. Elem.*, 33, 25-34

[10] Padron, L, A. Aznarez, J, J. and Maeso, O. (2011). 3-D Boundary Element – Finite Element Method for the Dynamic Analysis of Piled Buildings. *Eng. Anal. Bound. Elem.*, 35, 465-477

[11] Lysmer, J. Udaka, T. Seed, H. B. and Hwang, R.N. (1975). FLUSH a computer program for approximate 3-D analysis of soil-structure interaction problems. *Report No. EERC75-30*, University of California, Berkeley

[12] Lysmer, J. Udaka, T. Tsai, C.-F. and Seed, H. B. (1975). ALUSH a computer program for seismic response analysis of axisymmetric soil-structure systems. *Report No. EERC75-31*, University of California, Berkeley

[13] Fattah, M, Y. Schanz, T. and Dawood, S, H. (2012). The Role of Transmitting Boundaries in Modeling Dynamic Soil-Structure Interaction Problems. *Int. J. Engineering and Technology*, 2(2), 236-258

[14] Nakamura, N. (2006). Improved Methods to Transform Frequency Dependent Complex Stiffness to Time Domain. *Earthquake Engineering and Structural Dynamics*, 35, 1037-1050

[15] Nakamura, N. (2009). Nonlinear Response Analysis of Soil-Structure Interaction System Using Transformed Energy Transmitting Boundary in the Time Domain. *Soil Dynamics and Earthquake Engineering*, 29, 799-808

[16] Nakamura, N. (2012). Two-Dimensional Energy Transmitting Boundary in the Time Domain. *Int. J. Earhquakes and Strucures*, Vol.3, Numbr.2, pp.97-116

[17] Nakamura, N. (2012). Earthquake Response Analysis Using Nonlinear Energy Transmitting Boundary, Paper No. 1367, *Proc. 15WCEE (15th World Conference on Earthquake Engineering),* Lisboan, Portugal.

[18] Nakamura, N. (2015). Three Dimensional Energy Transmitting Boundary in the Time Domain. Frontiers, Built Environment, http://dx.doi.org/10.3389/fbuil.2015.00021, 2015.11

[19] Lysmer, J. and Waas, G. (1972). Shear wave in plane infinite structures. J. Eng. Mech. Div., ASCE, 98, EM1, 85-105

[20] Nakamura N. (2007). Practical Causal Hysteretic Damping. *Earthquake Engineering and Structural Dynamics*, 36, 597-617

[21] Nakamura, N. (2012). A Basic Study on the Transform Method of Frequency Dependent Functions into Time Domain - Relation to Duhamel's integral and time domain transfer function—. *J. of Engineering Mechanics*, ASCE, 138(3), 276-285

[22] Schnabel, P. B., Lysmer, J. and Seed, H. B. (1972), SHAKE A Computer Program for Earthquake Response Analysis of Horizontally Layered Sites, *Report No.EERC72-12, University of California, Berkeley*